An Energy-Efficient NOMA for Small Cells in Heterogeneous CRAN Under QoS Constraints

Quoc-Tuan Vien[†], Tuan Anh Le[†], Ca V. Phan[‡], Michael Opoku Agyeman[§]
[†]School of Science and Technology, Middlesex University, United Kingdom. Email: {Q.Vien; T.Le}@mdx.ac.uk
[‡]Ho Chi Minh City University of Technology and Education, Vietnam. Email: capv@hcmute.edu.vn
[§]University of Northampton, United Kingdom. Email: Michael.OpokuAgyeman@northampton.ac.uk.

***Abstract*—This paper investigates downlink performance of wireless backhaul in a heterogeneous cloud radio access network (HCRAN) consisting of a cloud-based central station (CCS) and multi-tier small cells. Non-orthogonal multiple access (NOMA) is adopted for the downlink from the CCS to multiple small cells of different types (e.g. microcells, picocells and femtocells). Taking into account practical power consumption at small cells operating within various propagation environment models, we first develop a power allocation for the NOMA, which allows us to derive the energy efficiency (EE) of the wireless backhaul in the practical HCRAN downlink. It is shown that the NOMA is superior to the conventional OFDMA scheme achieving a higher EE of up to six times with the deployment of small cells. The propagation environment is also shown to have a significant impact on the EE performance with a big gap between different cell types when the number of cells is large. Particularly, the EE of the NOMA is shown to not always increase or decrease as a function of the number of cells, while the throughput performance at the cloud edge is strikingly degraded as the number of cells increases. This accordingly motivates us to propose a two-stage algorithm for determining the optimal number of various cells that maximises the EE of the HCRAN while still maintaining the QoS requirement at the cloud edge. Simulation results show that, to meet a target cloud-edge throughput, the same number of femtocells and picocells can be used; however, the femtocells are favourable to the picocells in achieving the maximal EE.**

I. Introduction

To find a way of dealing with a high demand of mobile users for the best quality-of-service (QoS), small cells have emerged as a means in prospective 5G communication systems to provide not only enhanced coverage but also improved network capacity for indoor and outdoor wireless services [1], [2]. With multiple overlaying layers or tiers, a heterogeneous wireless cellular network (HWCN), which consists of a mixture of macrocells, microcells, picocells and femtocells, was proposed for modelling modern cellular communications [3]–[6].

Along with HWCN, cloud radio access network (CRAN) has also attracted researchers as a novel solution enabling real-time cloud computing via centralised processing at the cloud to support base stations (BSs) in a number of services, such as interference management and handover control [7]. By employing CRAN architecture, the number of cell sites could be reduced and the burden of data processing and management at the BSs could be significantly lightened, which accordingly saves not only energy consumption but also operating costs towards a lower capital expenditure and green communications. Integrating the CRAN with the HWCN, a new network model, namely heterogeneous CRAN (HCRAN), was then developed, allowing the BSs in various cell types to be incorporated via a cloud, and thus could cooperatively assist the mobile users (e.g. in [8], [9] and references therein).

Investigating multiple access mechanisms, non-orthogonal multiple access (NOMA) is promising to be dominant in future radio access networks [10]–[12]. By exploiting the power domain rather than the traditional time and frequency domains, the NOMA can improve the spectral efficiency and network throughput of the downlink in wireless cellular networks. While the NOMA was shown to be beneficial compared to the OFDMA, to the best of the authors' knowledge, its energy efficiency (EE) when applying for small cells in a practical HCRAN and resource allocation for achieving maximal EE subject to QoS constraints have not been well investigated in the literature.

To this extent, in this paper, we investigate the application of NOMA for small cells in the downlink of HCRAN. In the proposed NOMA, a power allocation scheme is developed for BSs in various small cells (i.e. microcells, femtocells and picocells) according to the relative distances and the channel quality of the wireless links between them and the cloud-based central station (CCS). We then analyse the EE of the NOMA for small cells taking into account the power consumption at BSs in various cell types and the backhauling power consumption in heterogeneous network deployment as well as propagation environment model. It is shown that the NOMA scheme achieves a significantly improved performance compared to the conventional OFDMA scheme when deploying for small cells. The EE performance is also shown to be considerably affected by the propagation environment depending on the cell types and their quantity in the HCRAN.

In particular, the EE of NOMA is shown to vary, but not always increase or decrease, as a function of the number of cells, while the throughput performance at the cloud edge of HCRAN is noticeably degraded as the number of cells increases. It is therefore vital to find the optimal number of cells in the HCRAN to achieve the maximal EE while still supporting the cells at the cloud edge. As a second contribution of this paper, we propose a two-stage algorithm to find the optimal number of cells so as to maximise the EE subject to limited total power supply at the CCS, limited number of cells that can be supported and QoS constraint of cloud-edge throughput demands.

II. System Model of HCRAN Downlink

The system model of a HCRAN under investigation consists of K cell types (e.g. microcells, picocells, femtocells, etc.), each of which has N_k cells, $k = 1, 2, \ldots, K$, and the corresponding BS of the i_k-th cell, $i_k = 1, 2, \ldots, N_k$, is denoted by $\mathcal{BS}_{k,i_k}$. There is a CCS to manage the whole network via wireless bachaul links, which are assumed to experience Rayleigh flat fading. It is also assumed that the CCS transmits data to $\mathcal{BS}_{k,i_k}$ with a transmission power of $P_{k,i_k}^{(CCS)}$ and a transmission bandwidth of W. The BSs of the same cell type are assumed to have the same power consumption $P_k^{(BS)}$ with identical interfaces and switches.

Considering a practical HCRAN downlink, it is noted that the total power consumption in the whole network consists of not only the power consumption of all BSs in various cells and CCS, but also the power consumed by the wireless backhaul [9], [13], [14], which can be modelled as follows:

- *Power consumption of a BS*:

In order to run a practical wireless network, a BS basically requires power for signal processing at baseband (BB) unit, radio frequency (RF) transceiver and power amplifier (PA). Besides, there exist power losses caused by DC-DC power supply, mains supply (MS), cooling and inefficiency of the PA, which need to be considered in practice [15], [16]. Let us denote $P_k^{(A)}$, $P_k^{(RF)}$ and $P_k^{(BB)}$, $k = 1, 2, \ldots, K$, as the output radiated power at an antenna element, the RF power and the BB power, respectively, $N_k^{(T)}$ as the number of transceiver chains, $\eta_k^{(PA)}$ as the efficiency of the PA, $\alpha_k^{(feed)}$ as the feeder loss, $\alpha_k^{(DC)}$ as the DC-DC power supply loss, $\alpha_k^{(MS)}$ as the MS loss and $\alpha_k^{(cool)}$ as the cooling loss at the BS of the k-th cell type. The power consumption of the k-th type BS, i.e. $P_k^{(BS)}$, can be given by [15]

$$P_k^{(BS)} = N_k^{(T)} \frac{\frac{P_k^{(A)}}{\eta_k^{(PA)}\left(1-\alpha_k^{(feed)}\right)} + P_k^{(RF)} + P_k^{(BB)}}{\left(1-\alpha_k^{(DC)}\right)\left(1-\alpha_k^{(MS)}\right)\left(1-\alpha_k^{(cool)}\right)}. \tag{1}$$

- *Backhauling power*:

The power for the wireless backhaul includes the power consumption of downlink interfaces of wireless switches and aggregation switch in the CCS [13]. Let us denote $N_k^{(INT)}$, $k = 1, 2, \ldots, K$, as the number of interfaces per switch, $P_{k,\max}^{(SW)}$ as the maximum power consumption of a switch when all interfaces are used, $P_k^{(INT)}$ as the power consumption of an interface in the aggregation switch, $Ag_k^{(SW)}$ as the amount of traffic passing through a switch and $Ag_{k,\max}$ as the maximum amount of traffic that a switch at the k-th type BS can handle. The backhauling power for the downlink from CCS to the k-th type BS, i.e. $P_k^{(BH)}$, can be computed by [13]

$$P_k^{(BH)} = \frac{\omega_k P_{k,\max}^{(SW)} + (1-\omega_k)\frac{Ag_k^{(SW)}}{Ag_{k,\max}} P_{k,\max}^{(SW)}}{N_k^{(INT)}} + P_k^{(INT)}, \tag{2}$$

where ω_k is a weighting factor representing the relative influence between the maximal power consumption for the backplane of the switch, i.e. $P_{k,\max}^{(SW)}$, and the power quantity with respect to the amount of traffic passing through the switch, i.e. $Ag_k^{(SW)}$ [14].

Overall, the total power consumption for the HCRAN downlink can be determined by

$$P_{tot} = \sum_{k=1}^{K}\left[N_k\left(P_k^{(BS)} + P_k^{(BH)}\right) + \sum_{i_k=1}^{N_k} P_{k,i_k}^{(CCS)}\right]. \tag{3}$$

III. Power Allocation for NOMA

In HCRAN downlink employing NOMA, the signals $\{x_{k,i_k}\}$, $k = 1, 2, \ldots, K$, $i_k = 1, 2, \ldots, N_k$, for $\{\mathcal{BS}_{k,i_k}\}$ are superimposed at CCS as

$$x = \sum_{k=1}^{K}\sum_{i_k=1}^{N_k}\sqrt{P_{k,i_k}^{(CCS)}}\, x_{k,i_k}. \tag{4}$$

Over the fading channel, the signal received at the $\mathcal{BS}_{k,i_k}$, i.e. y_{k,i_k}, is given by

$$\begin{aligned} y_{k,i_k} &= h_{k,i_k}x + n_{k,i_k} \\ &= \sum_{k=1}^{K}\sum_{i_k=1}^{N_k}\sqrt{P_{k,i_k}^{(CCS)}}\, h_{k,i_k}x_{k,i_k} + n_{k,i_k}, \end{aligned} \tag{5}$$

where h_{k,i_k} is fading coefficient of the link CCS $\rightarrow$ BS$_{k,i_k}$ and n_{k,i_k} is additive white Gaussian noise at $\mathcal{BS}_{k,i_k}$ having zero mean and variance of σ_{k,i_k}^2.

In this paper, the wireless backhaul link CCS $\rightarrow$ BS$_{k,i_k}$, $k = 1, 2, \ldots, K$, $i_k = 1, 2, \ldots, N_k$, is assumed to experience Rayleigh flat fading channel with $E[|h_{k,i_k}|^2] = 1/d_{k,i_k}^{\nu_{k,i_k}}$, where $E[\cdot]$ denotes the statistical expectation function, d_{k,i_k} denotes the distance between BS$_{k,i_k}$ and CCS, and ν_{k,i_k} denotes the path loss exponent of the propagation model. Let G_{k,i_k} denote the normalised channel gain of the link CCS $\rightarrow$ BS$_{k,i_k}$ over the noise power, i.e.

$$G_{k,i_k} = \frac{E[|h_{k,i_k}|^2]}{\sigma_{k,i_k}^2} = \frac{1}{d_{k,i_k}^{\nu_{k,i_k}}\sigma_{k,i_k}^2}. \tag{6}$$

It can be noticed in (6) that both the distance, i.e. d_{k,i_k}, and the wireless channel propagation model, i.e. ν_{k,i_k}, between CCS and BS$_{k,i_k}$ have considerable impacts on G_{k,i_k}, which accordingly affects the power allocation for NOMA in HCRAN downlink.

For simplicity, the noises at the BSs of the same cell type are assumed to have the same power, i.e. $\sigma_{k,i_k}^2 = \sigma_{k,0}^2$, $\forall k = 1, 2, \ldots, K$, $i_k = 1, 2, \ldots, N_k$. Let us consider the power allocation for the BSs in the k-th type cells[1] and let $P_{k,tot}^{(CCS)}$, $k = 1, 2, \ldots, K$, denote the total transmission power at the CCS for BSs in k-th type cells, i.e.

$$P_{k,tot}^{(CCS)} = \sum_{i_k=1}^{N_k} P_{k,i_k}^{(CCS)}. \tag{7}$$

At BSs, successive interference cancellation (SIC) technique is employed to recover the interested data in a decreasing order of the channel gain where the BS having a higher channel gain is decoded before the one with a lower

[1]Note that the power allocation for the whole network can be straightforwardly obtained by individually treating BSs of the same cell type.

channel gain. Without loss of generality, let us assume that $G_{k,1} > G_{k,2} > \cdots > G_{k,N_k}$. The power allocated at the BSs in k-th type cells should therefore satisfy $P_{k,1}^{(CCS)} < P_{k,2}^{(CCS)} < \cdots < P_{k,N_k}^{(CCS)}$, which can be approximately assumed to be inversely proportional to the channel gains. Let λ_{k,i_k}, $i_k = 1, 2, \ldots, N_k - 1$, denote the ratio of power allocated for BS_{k,i_k+1} and the power for BS_{k,i_k}, i.e.

$$\lambda_{k,i_k} = \frac{P_{k,i_k+1}^{(CCS)}}{P_{k,i_k}^{(CCS)}} \approx \frac{G_{k,i_k}}{G_{k,i_k+1}} = \frac{d_{k,i_k+1}^{\nu_{k,i_k+1}}}{d_{k,i_k}^{\nu_{k,i_k}}}. \tag{8}$$

Recursively, $P_{k,i_k+1}^{(CCS)}$ in (8) can be determined by

$$\begin{aligned} P_{k,i_k+1}^{(CCS)} &= \lambda_{k,i_k} P_{k,i_k}^{(CCS)} \\ &= \lambda_{k,i_k}\lambda_{k,i_k-1} P_{k,i_k-1}^{(CCS)} \\ &= \prod_{j=1}^{i_k} \lambda_{k,j} P_{k,1}^{(CCS)}. \end{aligned} \tag{9}$$

The total transmission power at the CCS for BSs in k-th type cells can be obtained by

$$P_{k,tot}^{(CCS)} = \sum_{i_k=1}^{N_k} \prod_{j=1}^{i_k-1} \lambda_{k,j} P_{k,1}^{(CCS)}. \tag{10}$$

The power for $\text{BS}_{k,1}$ can be therefore allocated as

$$P_{k,1}^{(CCS)} = \frac{P_{k,tot}^{(CCS)}}{\sum_{i_k=1}^{N_k} \prod_{j=1}^{i_k-1} \lambda_{k,j}}. \tag{11}$$

Substituting (11) into (9), the power for other BSs, i.e. BS_{k,i_k}, $i_k = 2, 3, \ldots, N_k$, can be sequentially determined as

$$P_{k,i_k}^{(CCS)} = \frac{\prod_{j=1}^{i_k-1} \lambda_{k,j}}{\sum_{i_k=1}^{N_k} \prod_{j=1}^{i_k-1} \lambda_{k,j}} P_{k,tot}^{(CCS)}. \tag{12}$$

IV. Energy Efficiency of NOMA

In this section, we derive the EE of NOMA for small cells in HCRAN downlink. The EE is defined as the ratio of the total achievable throughput and the total power consumption required for the wireless backhaul downlink. Let τ_{tot} [bits/sec] and ξ [bits/Joule] denote the total throughput and the EE, respectively. ξ can be given by

$$\xi \triangleq \frac{\tau_{tot}}{P_{tot}}, \tag{13}$$

where P_{tot} is computed by (3). Let τ_{k,i_k} [bits/sec], $k = 1, 2, \ldots, K$, $i_k = 1, 2, \ldots, N_k$, denote the achievable throughput at BS_{k,i_k}. Applying NOMA with SIC technique over the power domain, τ_{k,i_k} can be derived as

$$\tau_{k,i_k} = W \log_2 \left(1 + \frac{P_{k,i_k}^{(CCS)} |h_{k,i_k}|^2}{\sum_{j=1}^{i_k-1} P_{k,j}^{(CCS)} |h_{k,j}|^2 + \sigma_k^2} \right). \tag{14}$$

The total achievable throughput is thus given by

$$\tau_{tot} = \sum_{k=1}^{K} \sum_{i_k=1}^{N_k} W \log_2 \left(1 + \frac{P_{k,i_k}^{(CCS)} |h_{k,i_k}|^2}{\sum_{j=1}^{i_k-1} P_{k,j}^{(CCS)} |h_{k,j}|^2 + \sigma_k^2} \right). \tag{15}$$

Substituting (15) and (3) into (13), we obtain

$$\xi = \frac{\sum_{k=1}^{K} \sum_{i_k=1}^{N_k} W \log_2 \left(1 + \frac{P_{k,i_k}^{(CCS)} |h_{k,i_k}|^2}{\sum_{j=1}^{i_k-1} P_{k,j}^{(CCS)} |h_{k,j}|^2 + \sigma_k^2} \right)}{\sum_{k=1}^{K} \left[N_k \left(P_k^{(C)} + P_k^{(BH)} \right) + \sum_{i_k=1}^{N_k} P_{k,i_k}^{(CCS)} \right]}. \tag{16}$$

Remark 1 (*Performance comparison between NOMA and OFDMA*)**.** Employing the conventional OFDMA for HCRAN downlink, the achievable throughput at the BS_{k,i_k}, $k = 1, 2, \ldots, K$, $i_k = 1, 2, \ldots, N_k$, is given by

$$\tau_{k,i_k}^{(\text{OFDMA})} = W \beta_{k,i_k} \log_2 \left(1 + \frac{P_{k,i_k}^{(CCS)} |h_{k,i_k}|^2}{\beta_{k,i_k} \sigma_k^2} \right), \tag{17}$$

where β_{k,i_k} ($0 < \beta_{k,i_k} < 1$) denotes the ratio of bandwidth sharing for BS_{k,i_k} having $\sum_{k=1}^{K} \sum_{i_k=1}^{N_k} \beta_{k,i_k} = 1$. Similarly, the EE of the OFDMA can be determined by

$$\xi^{(OFDMA)} = \frac{\sum_{k=1}^{K} \sum_{i_k=1}^{N_k} W \beta_{k,i_k} \log_2 \left(1 + \frac{P_{k,i_k}^{(CCS)} |h_{k,i_k}|^2}{\beta_{k,i_k} \sigma_k^2} \right)}{\sum_{k=1}^{K} \left[N_k \left(P_k^{(C)} + P_k^{(BH)} \right) + \sum_{i_k=1}^{N_k} P_{k,i_k}^{(CCS)} \right]}. \tag{18}$$

Note that NOMA has been shown to achieve a higher throughput than the conventional OFDMA [10]. From (16) and (18), given the same total power consumption in the whole network, a higher EE is therefore achieved with the NOMA over the OFDMA.

V. Energy Efficiency Optimisation for NOMA

It can be noticed in (16) that the EE of NOMA depends on the number of cells of different types and their power allocation, especially at the cloud edge where the cells are far away from the CCS.

Specifically, as shown later in the numerical results, depending on the cell types, either a very small number or a very large number of cells may cause a very poor EE performance. Also, given a fixed total power available at CCS, it can be intuitively observed that the throughput of cells at the cloud edge is considerably degraded as the number of cells increases. This means the number of cells that can be supported is limited and the EE could be maximised at a certain number of cells within the coverage of the CCS.

Therefore, subject to the QoS constraints of cloud-edge throughput and limited total power available at CCS, the EE optimisation problem can be formulated as follows:

$$\max_{N_1, N_2, \ldots, N_K} \xi \tag{19}$$

s.t.

$$\sum_{k=1}^{K} \sum_{i_k=1}^{N_k} P_{k,i_k}^{(CCS)} \leqslant P_{\max}^{(CCS)}, \tag{20}$$

$$\tau_{k,N_k} \geq \tau_{k,thre}, \forall k = 1, 2, \ldots, K, \tag{21}$$

$$N_k \leqslant N_{k,\max}, \forall k = 1, 2, \ldots, K, \tag{22}$$

where ξ is given by (16), $P_{\max}^{(CCS)}$ is the maximum power available at CCS, $\tau_{k,thre}$ is the cloud-edge throughput thresh-

old, $N_{k,\max}$ is the maximum number of k-th type cells in the HCRAN and τ_{k,N_k} is the throughput at BS_{k,N_k} of the k-th cell type at cloud edge (see (14)).

In order to solve the optimisation problem in (19), it can be observed that the optimal number of cells in the whole network can be determined by separately dealing with each cell type given the constraint on the maximum power available for each cell type. The optimisation problem in (19) can thus be rewritten as

$$\max_{\{N_k\}} \frac{\sum_{i_k=1}^{N_k} W \log_2 \left(1+\frac{P_{k,i_k}^{(CCS)}|h_{k,i_k}|^2}{\sum_{j=1}^{i_k-1} P_{k,j}^{(CCS)}|h_{k,j}|^2+\sigma_k^2}\right)}{N_k\left(P_k^{(C)}+P_k^{(BH)}\right)+\sum_{i_k=1}^{N_k} P_{k,i_k}^{(CCS)}} \tag{23}$$

s.t. (21), (22),

$$\sum_{i_k=1}^{N_k} P_{k,i_k}^{(CCS)} \leqslant P_{k,\max}^{(CCS)}, \tag{24}$$

$$\sum_{k=1}^{K} P_{k,max}^{(CCS)} = P_{\max}^{(CCS)}, \tag{25}$$

where $P_{k,\max}^{(CCS)}$ is the maximum power allocated for the BSs of k-th type cells and the constraint in (25) is added in accordance with the limited total power in the whole network.

Remark 2 (*Motivation for the proposal of a two-stage algorithm*)**.** Note that the throughput of cells at the cloud edge decreases as the number of cells increases. Therefore, in order to meet the QoS constraint of the cloud-edge throughput requirement in (21), it is crucial to firstly find out the maximum number of cells of each type that can be supported given the limited number of cells in (22) and the limited available power in (24) and (25). Then, among these maximum cell ranges, the optimal number of cells for maximising EE can be correspondingly determined.

From the above observation in Remark 2, the optimisation problem in (23) can be solved in two stages as follows:

- *Stage 1*: Find the maximum number of cells by solving

$$\max N_k \tag{26}$$

s.t. (21), (22) and (24).

Let $N_{k,\max}^{(1)}$ denote the maximum number of the k-th type cells after stage 1. The EE $\xi_k^{(1)}$ w.r.t. $N_{k,\max}^{(1)}$ is

$$\xi_k^{(1)} = \frac{\sum_{i_k=1}^{N_{k,\max}^{(1)}} W \log_2 \left(1+\frac{P_{k,i_k}^{(CCS)}|h_{k,i_k}|^2}{\sum_{j=1}^{i_k-1} P_{k,j}^{(CCS)}|h_{k,j}|^2+\sigma_k^2}\right)}{N_{k,\max}^{(1)}\left(P_k^{(C)}+P_k^{(BH)}\right)+\sum_{i_k=1}^{N_{k,\max}^{(1)}} P_{k,i_k}^{(CCS)}} \tag{27}$$

Note that, after Stage 1, the constraints of cloud-edge throughput and limited power in (21) and (24) can be relaxed, while the constraint of the limited number of cells in (22) is now stricter with

$$N_k \leqslant N_{k,\max}^{(1)}. \tag{28}$$

- *Stage 2*: Find the optimal number of cells in the range of $[1, N_{k,\max}^{(1)}]$ to maximise the EE in (23), i.e.

$$\max_{N_k \in [1, N_{k,\max}^{(1)}]} \xi_k, \tag{29}$$

where ξ_k denotes the objective function in (23). The optimal number of the k-th type cells after Stage 2 and its corresponding maximal EE are denoted by $N_{k,opt}^{(2)}$ and $\xi_{k,\max}^{(2)}$, respectively.

The finding of the optimal number of cells for NOMA in HCRAN using the above two stages can be realised with an iterative searching algorithm as summarised in Algorithm 1.

Algorithm 1 Optimal number of cells for NOMA in HCRAN

for $k = 1$ **to** K **do**
  STAGE 1:
  $N_{k,\max}^{(1)} \leftarrow 0$
  $j \leftarrow 0$
  repeat
    $j \leftarrow j + 1$
    Find $\{P_{k,i_k}^{(CCS)}\}$, $i_k = 1, 2, \ldots, j$, using (12).
    Find $\tau_{k,j}$ using (14).
  until $\tau_{k,j} < \tau_{k,thre}$ **or** $j > N_{k,\max}$
  $N_{k,\max}^{(1)} \leftarrow j - 1$
  STAGE 2:
  $N_{k,opt}^{(2)} \leftarrow 0$, $\xi_{k,\max}^{(2)} \leftarrow 0$
  for $j = 1$ **to** $N_{k,\max}^{(1)}$ **do**
    Find ξ_k in (23) using $\{P_{k,i_k}^{(CCS)}\}$, $i_k = 1, 2, \ldots, j$, determined in Stage 1.
    if $\xi_k \geqslant \xi_{k,\max}^{(2)}$ **then**
      $N_{k,opt}^{(2)} \leftarrow j$
      $\xi_{k,\max}^{(2)} \leftarrow \xi_k$
    else
      break (End of Stage 2 for k-th cell type)
    end if
  end for
end for

Remark 3 (*Lower number of cells for higher cloud-edge throughput*)**.** From the QoS constraint of cloud-edge throughput requirement in (21) in Stage 1 of Algorithm 1, it can be shown that $N_{k,\max}^{(1)}$, $k = 1, 2, \ldots, K$, monotonically decreases over $\tau_{k,thre}$. Therefore, in order to provide a higher cloud-edge throughput for the HCRAN downlink, a lower number of cells is required.

VI. Numerical Results

In this section, the numerical results of EE of the proposed NOMA for small cells in HCRAN downlink are first presented, followed by the finding of the optimal number of cells using the proposed two-stage iterative searching in Algorithm 1. Specifically, three cell types, including microcells, picocells and femtocells, and two propagation environment models, including indoors (i.e. $\nu = 2.7$) and outdoors (i.e. $\nu = 3$), are considered.

The power consumption of various cell types is determined using (1) with simulation parameters in [15]. We

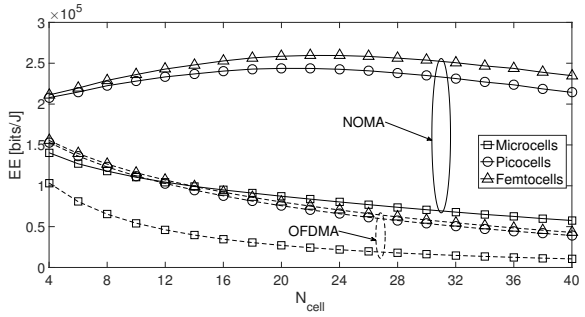

Fig. 1: EE of NOMA and OFDMA versus number of cells of various types.

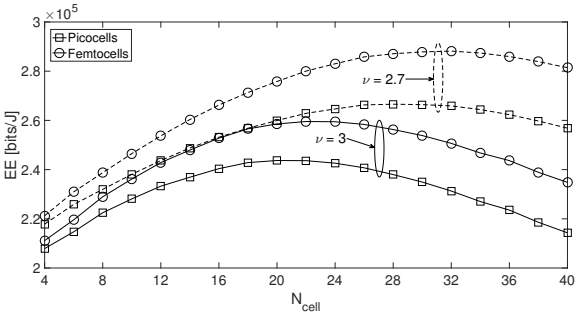

Fig. 2: EE of NOMA versus number of cells in various propagation environment.

can obtain $P^{(BS)}_{microcell} = 308.9$ W, $P^{(BS)}_{picocell} = 46.4$ W and $P^{(BS)}_{femtocell} = 37.9$ W. For the wireless backhaul, it is assumed that each switch has 24 interfaces with a maximum power consumption of 300 W, the power consumption of a downlink interface in the aggregation switch is 1 W, weighting factor is 0.5 and the maximum amount of traffic that can be handled is 24 Gbits/s.

A. EE of NOMA versus OFDMA for Small Cells in HCRAN

Figure 1 illustrates the EE of NOMA and OFDMA in HCRAN downlink as a function of the number of cells. It is assumed that there are a maximum of 40 small cells which are uniformly located outdoors within the range of 10 metres to 800 metres from CCS, the channel gains of the links from the CCS to the cells vary from 0 dB to 20 dB which are inversely proportional to their corresponding distances, the total transmission power available at the CCS is 1 kW and the transmission bandwidth is 10 MHz. It can be seen in Fig. 1 that, applying the NOMA for small cells results in a much improved EE performance of up to six times compared to the OFDMA. This accordingly confirms the statement in Remark 1 regarding a higher EE with NOMA. In particular, it can be noticed in Fig. 1 that the EE of the NOMA does not always increase or decrease as the number of cell increases, but there exists a certain number of femtocells and picocells that maximise the EE, which motivates us to propose an optimisation problem as described in Section V. Furthermore, the deployment of femtocells and picocells is shown to achieve a much better EE compared to microcells due to their lower power consumption, and thus in the following, let us consider the application of NOMA only for femtocells and picocells.

B. Impacts of Propagation Environment

Investigating the impacts of propagation environment on the performance of NOMA for small cells in HCRAN downlink, Fig. 2 plots the EE of the NOMA for femtocells and picocells against the number of cells with respect to various path loss exponents. Both indoor and outdoor environment are considered, while the other simulation parameters are similarly set as in Fig. 1. It can be observed in Fig. 2 that the EE of the NOMA for indoor cells is much higher than that for outdoor cells and the femtocells are shown to achieve a better performance than the picocells in both environment. Moreover, the EE is shown to reach its optimal value at a certain number of cells depending on the propagation models and cell types.

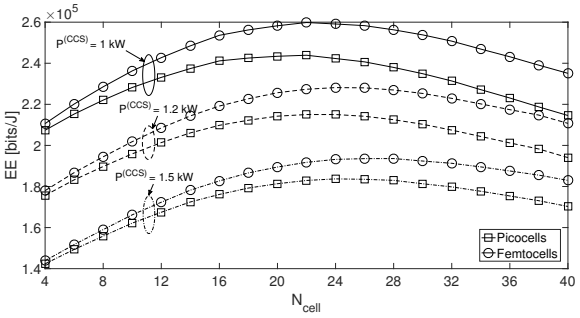

Fig. 3: EE of NOMA versus number of cells with various power available at CCS.

C. Impacts of Power Allocation at CCS

The impacts of power allocation at CCS on the performance of NOMA for HCRAN downlink are illustrated in Fig. 3 where the EE is plotted versus the number of cells with respect to different values of power available at the CCS. Specifically, three scenarios of $P^{(CCS)} = \{1, 1.2, 1.5\}$ kW are considered for femtocells and picocells which are located outdoors with $\nu = 3$. With similar settings as in Fig. 2, it can be noticed that a lower power is required at the CCS for femtocells to achieve the same throughput as with the picocells, and thus results in a higher EE performance. Also, a higher power supply at the CCS is shown to be unnecessary in terms of the EE, while a lower power supply is able to cover all cells. Similarly, the EE can achieve its maximal performance at a specific number of cells according to the power available at the CCS.

D. Optimal Number of Cells for NOMA in HCRAN

Finding the optimal number of cells in HCRAN, Fig. 4 illustrates the maximal number of cells (i.e. $N^{(1)}_{\max}$) as a function of cloud-edge throughput requirement (i.e. τ_{thre}). The maximal number of cells is determined by employing Stage 1 in Algorithm 1. The simulation parameters are similarly set as in Fig. 2 where femtocells and picocells are considered in both indoor and outdoor environment. It can be observed in Fig. 4 that an equal number of picocells and femtocells are restricted to achieve the same target cloud-edge throughput due to their approximately equal throughput. Also, the maximal number of cells is shown to

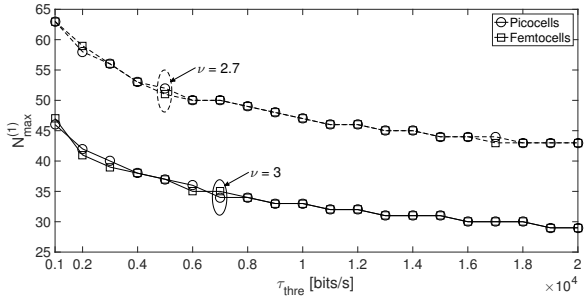

Fig. 4: Maximal number of cells versus target cloud-edge throughput in various propagation environment.

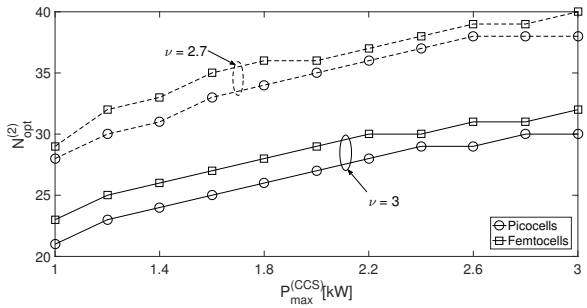

Fig. 5: Optimal number of cells versus total power available at CCS in various propagation environment.

decrease as the target cloud-edge throughput increases, which accordingly confirms the statement in Remark 3 in relation to the monotonic decreasing of the optimal number of cells over the cloud-edge throughput requirement.

Figs. 5 and 6 sequentially plot the optimal number of cells (i.e. $N^{(2)}_{opt}$) and the corresponding maximal EE (i.e. $EE^{(2)}_{\max}$) as functions of the maximum power available at CCS (i.e. $P^{(CCS)}_{\max}$). The results are obtained by applying Stage 2 of Algorithm 1 given the numerical results of the maximal number of cells from Stage 1 of Algorithm 1 (see Fig. 4). It can be observed that the optimal number of cells increases as the power at CCS increases and the indoor environment is shown to be able to support more cells with a higher maximal EE when compared to the outdoor environment. Furthermore, with a limited total power, a higher number of femtocells can be supported achieving a higher EE compared to that of the picocells due to the lower power consumption of the femtocells.

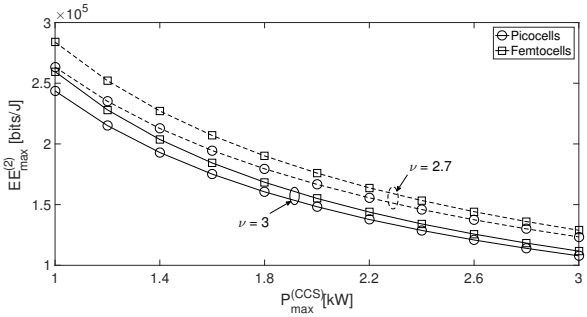

Fig. 6: Maximal EE versus total power available at CCS in various propagation environment.

VII. Conclusions

In this paper, an energy-efficient NOMA has been proposed for small cells in HCRAN downlink taking into account the practical power consumption of different cell types and wireless backhaul. Specifically, a power allocation scheme has been developed to allocate the power at various cell types. It has been shown that the NOMA scheme achieves an improved EE performance of up to six times over the conventional OFDMA scheme when deploying for small cells. Furthermore, a two-stage algorithm has been developed to find the optimal number of cells to maximise the EE of the HCRAN downlink while guaranteeing the cloud-edge throughput requirement. It has been shown that the same number of femtocells and picocells can be employed for a target cloud-edge throughput, while a higher number of femtocells are preferable to provide a higher EE.

References

[1] A. Ganz, C. Krishna, D. Tang, and Z. Haas, "On optimal design of multitier wireless cellular systems," *IEEE Commun. Mag.*, vol. 35, no. 2, pp. 88–93, Feb. 1997.

[2] J. Andrews, "Seven ways that HetNets are a cellular paradigm shift," *IEEE Commun. Mag.*, vol. 51, no. 3, pp. 136–144, Mar. 2013.

[3] T. A. Le and M. R. Nakhai, "Possible power-saving gains by dividing a cell into tiers of smaller cells," *Electron. Lett.*, vol. 46, no. 16, pp. 1163–1165, Aug. 2010.

[4] Q.-T. Vien, T. Akinbote, H. X. Nguyen, R. Trestian, and O. Gemikonakli, "On the coverage and power allocation for downlink in heterogeneous wireless cellular networks," in *Proc. IEEE ICC 2015*, London, UK, Jun. 2015, pp. 4641–4646.

[5] Q.-T. Vien, T. A. Le, H. X. Nguyen, and M. Karamanoglu, "An energy-efficient resource allocation for optimal downlink coverage in heterogeneous wireless cellular networks," in *Proc. IEEE ISWCS 2015*, Brussels, Belgium, Aug. 2015, pp. 156–160.

[6] T. E. Bogale and L. B. Le, "Massive MIMO and mmWave for 5G wireless HetNet: Potential benefits and challenges," *IEEE Veh. Technol. Mag.*, vol. 11, no. 1, pp. 64–75, Mar. 2016.

[7] J. Wu, Z. Zhang, Y. Hong, and Y. Wen, "Cloud radio access network (C-RAN): a primer," *IEEE Netw.*, vol. 29, no. 1, pp. 35–41, Jan. 2015.

[8] M. Peng, Y. Li, J. Jiang, J. Li, and C. Wang, "Heterogeneous cloud radio access networks: a new perspective for enhancing spectral and energy efficiencies," *IEEE Wireless Commun.*, vol. 21, no. 6, pp. 126–135, Dec. 2014.

[9] Q.-T. Vien, T. A. Le, B. Barn, and C. V. Phan, "Optimising energy efficiency of non-orthogonal multiple access for wireless backhaul in heterogeneous cloud radio access network," *IET Commun.*, vol. 10, no. 18, pp. 2516–2524, 2016.

[10] Y. Saito, Y. Kishiyama, A. Benjebbour, T. Nakamura, A. Li, and K. Higuchi, "Non-orthogonal multiple access (NOMA) for cellular future radio access," in *Proc. IEEE VTC 2013-Spring*, Dresden, Germany, Jun. 2013, pp. 1–5.

[11] L. Dai, B. Wang, Y. Yuan, S. Han, C. l. I, and Z. Wang, "Non-orthogonal multiple access for 5G: solutions, challenges, opportunities, and future research trends," *IEEE Commun. Mag.*, vol. 53, no. 9, pp. 74–81, Sep. 2015.

[12] Q.-T. Vien, N. Ogbonna, H. X. Nguyen, R. Trestian, and P. Shah, "Non-orthogonal multiple access for wireless downlink in cloud radio access networks," in *Proc. IEEE EW 2015*, Budapest, Hungary, May 2015, pp. 434–439.

[13] S. Tombaz, P. Monti, K. Wang, A. Vastberg, M. Forzati, and J. Zander, "Impact of backhauling power consumption on the deployment of heterogeneous mobile networks," in *Proc. IEEE GLOBECOM 2011*, Houston, TX, USA, Dec. 2011, pp. 1–5.

[14] O. Onireti, F. Heliot, and M. Imran, "On the energy efficiency-spectral efficiency trade-off of distributed MIMO systems," *IEEE Trans. Commun.*, vol. 61, no. 9, pp. 3741–3753, Sep. 2013.

[15] G. Auer, V. Giannini, C. Desset, I. Godor, P. Skillermark, M. Olsson, M. Imran, D. Sabella, M. Gonzalez, O. Blume, and A. Fehske, "How much energy is needed to run a wireless network?" *IEEE Wireless Commun.*, vol. 18, no. 5, pp. 40–49, Oct. 2011.

[16] B. H. Jung, H. Leem, and D. K. Sung, "Modeling of power consumption for macro-, micro-, and RRH-based base station architectures," in *Proc. IEEE VTC 2014-Spring*, Seoul, Korea, May 2014, pp. 1–5.